New Journal of Physics
The open access journal at the forefront of physics

Deutsche Physikalische Gesellschaft DPG IOP Institute of Physics

PAPER • OPEN ACCESS

Ab initio screening methodology applied to the search for new permanent magnetic materials

To cite this article: Nedko Drebov *et al* 2013 *New J. Phys.* **15** 125023

New Journal of Physics
The open access journal for physics

Ab initio screening methodology applied to the search for new permanent magnetic materials

Nedko Drebov[1,5], Alberto Martinez-Limia[2], Lothar Kunz[2], Adrien Gola[2], Takashi Shigematsu[3], Thomas Eckl[2], Peter Gumbsch[1,4] and Christian Elsässer[1,4,5]

[1] Fraunhofer Institute for Mechanics of Materials IWM, Wöhlerstraße 11, D-79108 Freiburg, Germany
[2] Corporate Sector Research and Advance Engineering, Robert Bosch GmbH, Postfach 10 60 50, D-70049 Stuttgart, Germany
[3] Research and Technology Center Asia Pacific, District Japan, Bosch Corporation, 3-6-7, Shibuya, Shibuya-ku, Tokyo 150-8360, Japan
[4] Karlsruhe Institute of Technology, Institute for Applied Materials (IAM-ZBS), Engelbert-Arnold-Straße 4, D-76131 Karlsruhe, Germany
E-mail: nedko.drebov@iwm.fraunhofer.de
and christian.elsaesser@iwm.fraunhofer.de

New Journal of Physics **15** (2013) 125023 (24pp)
Received 27 June 2013
Published 17 December 2013
Online at http://www.njp.org/
doi:10.1088/1367-2630/15/12/125023

Abstract. In this paper a computational high-throughput screening (HTS) approach to the search for alternative permanent magnetic materials is presented. Systems considered for a start are binary intermetallic compounds composed of rare-earth (RE) and transition metal (TM) elements. With the tight-binding-linear muffin-tin-orbital-atomic-sphere-approximation (TB-LMTO-ASA) method of density functional theory (DFT) a variety of RE–TM intermetallic phases is investigated and their magnetic properties are obtained at rather low computational costs. Next, interstitial elements such as boron, carbon and nitrogen in these phases are considered. For promising candidate phases with high and stable spontaneous ferromagnetic polarization, the calculated local magnetic moments and exchange coupling parameters, as

[5] Authors to whom any correspondence should be addressed.

obtained from TB-LMTO-ASA calculations, are then used for Monte Carlo simulations to identify candidates with sufficiently high Curie temperatures (T_c). Finally, magnetocrystalline anisotropy constants (K_1) of the most promising candidate phases are calculated with accurate, potential-shape-unrestricted DFT calculations using the Vienna *ab initio* simulation package. The computational HTS procedure is illustrated by results for a selection of hard-magnetic RE–TM phases like $RETM_5$, RE_2TM_{17} and $RE_2TM_{14}B$.

Contents

1. Introduction

In recent years of rapid developments in the fields of electro-mobility and renewable-energy technologies, permanent magnetic materials composed of rare-earth (RE) and transition-metal (TM) elements have become of major importance due to their wide range of applications as hard-magnetic RE–TM phases for permanent magnets in electrical motors and generators, and various other functional components. However, the discovery of $Nd_2Fe_{14}B$, which currently shares first place with Ba/Sr ferrites as the most used material for permanent magnets, dates back to 1984 (Croat *et al* 1984, Herbst *et al* 1984). Due to the limited resources of RE elements and a latent supply monopoly on the international market, the goal is to discover and develop new hard-magnetic materials with lower RE content (ultimately RE-free magnets) and improved hard-magnetic performance (Kramers *et al* 2012). It is the purpose of this work to propose a fast and efficient computational strategy for the search for such novel hard-magnetic materials.

In recent reviews, e.g. by Kramers *et al* (2012), Coey (2011, 2012) or Gutfleisch *et al* (2011), different prospects and perspectives for the development of hard magnetic materials are discussed and the current state in the experimental and theoretical characterization of such materials is described. The large quantity of permanent magnets needed in contemporary technology, especially with the increased interest in alternative energy sources, transmission and conversions, also causes ecological concerns and economic problems, which are discussed in details by Alonso *et al* (2012).

The systematic search for novel hard magnetic materials is hardly achievable only via experimental discovery due to the very large combinatorial space spanned by the crystal structures and chemical compositions for compounds of RE, TM and interstitial (IS) elements. This difficulty is also connected with eventually high and unstable costs of raw materials on the world market and the time-consuming procedures of synthesis and characterization. In a very recent paper by Curtarolo *et al* (2013) a way toward an automated and efficient computational materials-design procedure was reviewed, and among the different areas of applications discussed magnetic materials were considered. This high-throughput screening (HTS) procedure combines a first-principles method of density functional theory (DFT) for computing the magnetic and thermodynamic properties of materials with the development of a large database of material parameters and the application of data mining procedures (Curtarolo *et al* 2013).

It is of great importance for the theoretical search for hard-magnetic materials to gain detailed insight into the most relevant physical mechanisms which determine the intrinsic properties of the hard-magnetic materials (Fähnle *et al* 1993). These intrinsic properties are spontaneous magnetization M_s, Curie temperature T_c and magnetocrystalline anisotropy energy (MAE), the latter characterized by, e.g., the constants K_1 and K_2 for uniaxial anisotropy. These properties are determined by local magnetic moments, exchange and spin–orbit interactions of electronic states on the atomic level. From the theoretical point of view, one can compute the local and total magnetic moments, exchange interactions as well as anisotropy constants which can deliver reasonable estimates for the desired intrinsic properties of the magnetic materials.

In almost all modern hard-magnetic materials the intrinsic material parameters are achieved as desired (Buschow 1991, Coey 1996) by combining TM and RE elements in particular proportions. This results in a large class of possible chemical compositions and crystal structures. In these compounds, the RE partner with 4f electron states is responsible for the high magnetic anisotropy, whereas the TM partner with 3d electron bands is responsible for the large magnetic moment and the ferromagnetic coupling which ensures a high Curie temperature. It is therefore well established that combining these two types of elements one can get materials with both high magnetic anisotropy and high Curie temperature (Fähnle *et al* 1993).

There are several prerequisites for the candidates for novel intermetallic RE–TM compounds which have to be fulfilled in order to apply these materials as practical permanent magnets with high energy density (Coey 1996). The use of permanent magnets in high temperature applications requires the candidate materials to have a Curie temperature well above the $T_c = 590\,\mathrm{K}$ of $Nd_2Fe_{14}B$. The next important criterion concerns the magnetic anisotropy of intermetallic phases. To improve the anisotropy contribution of the crystal structure, preference is given to non-cubic, uniaxial-symmetry crystal structures such as tetragonal, rhombohedral or hexagonal ones. A positive anisotropy constant similar to the $K_1 = +4.9$ of $Nd_2Fe_{14}B$ (Coey 1996) is desired, so that the c-axis is the easy direction. Furthermore, a magnetic saturation polarization $J_s = \mu_0 M_s$ greater than 1.0 T should be achieved.

The purpose of this paper is to present a HTS procedure which assesses the computed local and total magnetic moments, exchange interactions as well as anisotropy constants in both a reasonably accurate and efficient manner to meet the above mentioned criteria for hard magnetic materials. The paper is organized as follows. In section 2 the computational procedure used for the investigation of permanent magnetic materials is described. In section 3 we present and discuss illustrative results for some common hard magnetic phases, namely $RETM_5$, $RE_2TM_{14}B$ and RE_2TM_{17}. The validation of the magnetic properties computed with the computationally fast but potential-shape-restricted tight-binding-linear muffin-tin-orbital-atomic-sphere-approximation (TB-LMTO-ASA) method by a potential-shape-unrestricted DFT method of high accuracy, namely the Vienna *ab initio* simulation package (VASP) (Kresse and Furthmüller 1996a, 1996b, Kresse and Joubert 1999), as well as computations of magnetic anisotropy, Curie temperature and phase stability of RE–TM compounds are presented in sections 4–7. A summary with some prospects for improvements of the proposed HTS methodology for the search for high-performance permanent magnetic materials concludes the paper.

2. Computational methods

The computational modeling and design of RE–TM intermetallic phases face three major problems associated with the nature of the constituting RE and TM elements and the choice of proper theoretical method. The first two problems were already described by Fähnle *et al* (1993) and are connected to: (i) the interplay between the localized magnetism of the 4f electrons of the RE atoms and the itinerant magnetism originating from 3d electrons of the TM atoms and (ii) the large unit cells, which have to be treated (in the case of $Nd_2Fe_{14}B$ the unit cell consists of four formula units or 68 atoms). The third problem is the computational time needed to perform the HTS procedure for the search of possible intermetallic phases due to the large combinatorial space spanned by the variety of distributing RE, TM and IS elements in crystal structures.

2.1. High-throughput density-functional-theory calculations of the magnetic properties

Since there is a plethora of potential crystal structures and chemical compositions, there is a need for a fast, efficient and automated HTS procedure to find permanent magnetic materials. As already mentioned in the introduction, a comprehensive description of HTS procedures was provided by Curtarolo *et al* (2013). The practical implementation of HTS methods is a highly non-trivial task. Many variations are possible which depend on the choice of the first-principles methods software packages used as well as the data mining approaches. In recent years, there are only a few papers so far addressing the application of the HTS procedures for the search of permanent magnetic materials. For instance, Gilleßen and Dronkowski (2009, 2010) performed an extended combinatorial study with DFT on a set of 810 normal and inverse full Heusler phases. The authors investigated the thermodynamic stability and the ferromagnetism of a large class of possible Heusler alloys and identified a number of so far unknown stable magnetic phases as candidates for high density memory storage devices. Related to this theoretical HTS work, the group of Felser *et al* studied the Heusler phases by experimental HTS methods, succeeded in synthesizing several promising hard-magnetic phases experimentally and thus confirmed some theoretical predictions (Winterlik *et al* 2012, Gasi *et al* 2013, Kiss *et al* 2013).

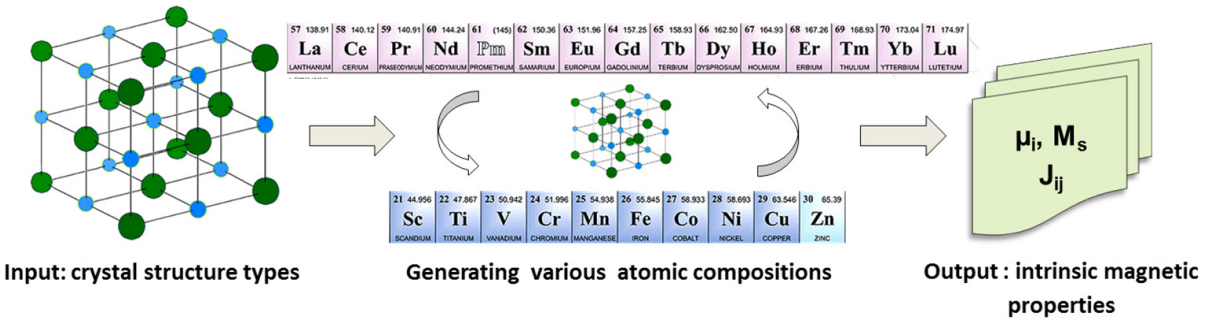

Figure 1. Work-flow diagram representing the automated HTS procedure for the search of new hard magnetic compounds.

The crucial step in the modeling of novel intermetallic RE–TM compounds as practical permanent magnets is to substitute the critical RE elements by other elements. This can be achieved by a systematic investigation of the magnetic properties of a large class of crystal structures and compositions. To tackle this problem, we have developed an automated HTS procedure to estimate the magnetic properties of RE–TM compounds. The work-flow diagram is shown in figure 1.

The HTS procedure starts with a given crystal structure selected from a database of known crystal structure types, which belong to, e.g., the family of topologically close-packed phases (Seiser *et al* 2011). For the selected crystal structure, various chemical compositions of the possible RE, TM and IS elements are generated and their intrinsic magnetic properties such as total and local magnetic moments, and exchange integrals are computed with the computationally fast TB-LMTO-ASA method. For most promising candidate phases, the anisotropy constants (K_1) and Curie temperatures (T_c) are then calculated in a subsequent step with the computationally accurate VASP code. All these computational tasks can be performed in an automated way more efficiently if one includes various restart options, the possibility for input-file correction as well as parallelization of TB-LMTO-ASA runs. The results of these HTS computations are compiled in a large materials database of intrinsic magnetic properties for intermetallic phases.

The crystal phases selected in this work ($RE_2TM_{14}B$, RE_2TM_{17} and $RETM_5$) to test the proposed HTS methodology cover a wide range of tetragonal, rhombohedral and hexagonal structure types. There exist further crystal structure types with RE:TM ratios like 1:12 and 3:29 which all can be derived from the basic hexagonal $CaCu_5$ structure (see figure 2) as described by Burzo *et al* (1990) and Rao *et al* (1999).

Our initial choice of elements was guided by the crustal abundance of the TM and RE elements and by the local magnetic moments of their elemental ferromagnetic phases. The most abundant and cheapest TM element is iron; it also possesses the largest local magnetic moment of 2.217 μ_B as present in bcc Fe (Skomski 2008). The most abundant RE elements are actually the 'light' ones with less than half-filled 4f electron shells, like cerium or neodymium. The magnetic moments of the light RE elements are oriented parallel to those of the TM (Blundell 2001). Therefore, for combinations of light RE elements and Fe, one expects larger magnetic moments of the constituting intermetallic phases. Although the 'heavy' RE elements have spins anti-parallel to those of the TM atoms and typically lead to lower total magnetic moments, their addition can increase the Curie temperature (Blundell 2001).

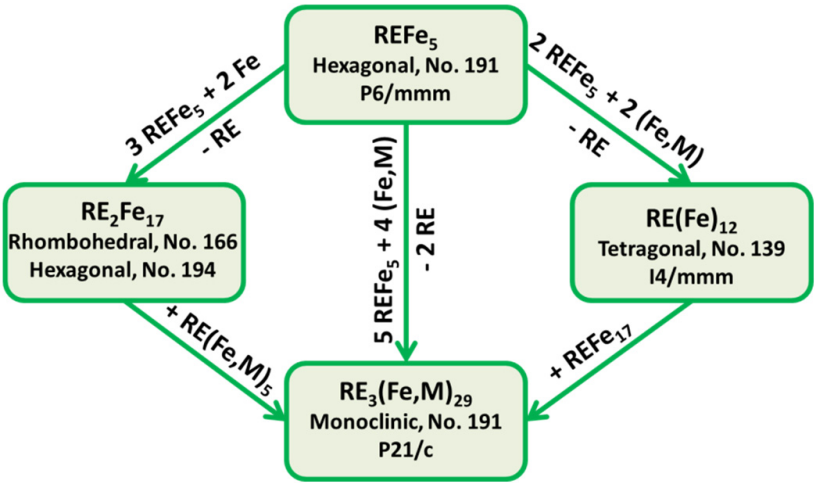

Figure 2. Schematic representation of the structural interrelationships of RE–TM phases with RE:TM ratios 1:5, 1:12, 2:17 and 3:29.

2.2. Fast computation of magnetic properties with the tight-binding-linear muffin-tin-orbital-atomic-sphere-approximation method

For the fast computation of the intrinsic magnetic properties of the magnetic materials, we use the LMTO method (Andersen 1975) in the ASA with the TB representation of LMTOs (Andersen and Jepsen 1984). All calculations were performed within the framework of the local-spin density approximation (LSDA) using a minimal spd basis set of LMTOs and the exchange-correlation functional of von Barth and Hedin (1972) in the parameterization of Moruzzi *et al* (1978). The ASA is a potential-shape approximation, for which the crystal is subdivided into space-filling and therefore slightly overlapping atomic spheres (the total unit-cell volume is equal to the sum of atomic-sphere volumes). Inside each sphere the effective crystal potential has spherical symmetry. This method yields accurate results for many physical quantities as long as the overlap of the atomic spheres is small, as in close-packed metals. In the choice of atomic-sphere radii for the different sets of RE, TM and IS elements, we rely on previous experience (Beuerle and Fähnle 1992) that the ratio of r(RE):r(TM):r(IS) = 1.35:1.00:0.70 yields results for magnetic properties which are very close to experimental ones.

Since the LSDA is valid for weakly correlated systems and the RE–TM systems have more strongly correlated, localized f-electrons in addition to delocalized d-electrons, the f-electrons are treated in the so called 'open-core' approximation (Brooks *et al* 1991a, 1991b), by imposing two constraints for the 4f charge and spin density entering the effective potential in LSDA. Within this approximation, one explicitly does not allow direct hybridization of f-electron states with other valence-electron states but we simulate the effect of 4f states below the valence band by imposing a non-zero logarithmic derivative to the radial 4f wave-functions at the atomic-sphere surfaces of the RE atoms. The constraint for the charge density fixes the number of electrons in the 4f core to the one of a free RE^{3+} ion. The constraint for the spin density fixes the magnetic spin moment of the 4f core to the value obtained from the atomic Russell–Saunders coupling for the projection of the free-ion 4f spin moment along the direction of the total 4f moment. In this way the strong Hund's rule correlations in the 4f shells are approximately accounted for. The magnetic moments calculated with the Russell–Saunders coupling often

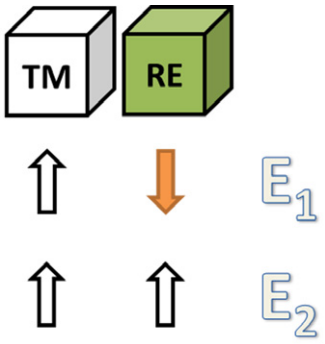

Figure 3. The two possible spins states of the two-sublattice model for a ferromagnetic RE–TM phase with only one crystallographic site for the RE element.

agree with experiment, although crystal-field splittings may also alter the moments. Although the interaction between the magnetism of the valence-band states and that of the 4f states occurs through the local exchange-correlation potential, there will effectively be a coupling between the RE 4f and TM 3d states in RE–TM compounds via hybridization between the RE 5d and TM 3d states (Brooks *et al* 1991a, 1991b). The corresponding numbers of spin-up and spin-down f-electrons used in the TB-LMTO-ASA calculations according to the frozen-core approximation can be found in Liebs (1992) and Blundell (2001).

Besides the total and local magnetic moments, we are also interested in the exchange parameters as quantities for comparison with experimental results and phenomenological models (Coey 1996), and particularly as model parameters for Monte Carlo simulations to determine critical temperatures (see section 6). To compute the exchange couplings in the RE–TM intermetallics we use the so called two-sublattice model (Fähnle *et al* 1993). Within this model, one divides the crystal lattice into two sublattices, one composed of RE elements and the other of TM elements only (see figure 2). If the crystal structure of interest has only one crystallographic site for RE atoms, there are two spin states with energies E_1 and E_2 (see figure 3) which need to be computed for every stoichiometry to get an estimate for the J_{RT} integrals according to

$$J_{RT} = \frac{E_1 - E_2}{4 S_R \bar{S}_T Z_{RT} Z_R}, \tag{1}$$

where E_1 and E_2 are the total energies of the parallel and antiparallel spin states (see figure 3), S_R is the magnetic spin moment of the RE sublattice, S_T is the averaged magnetic spin moment of the TM sublattice, Z_{RT} is the number of nearest neighboring TM atoms around the RE atom and Z_R is the number of RE elements in the unit cell.

The determination of J_{RT} is important for the following reasons (Fähnle *et al* 1993): (i) J_{RT} is responsible for the transfer of the strong RE magneto-crystalline anisotropy to the TM sublattice due to the crystal-field coupling; (ii) at high temperatures J_{RT} contributes to the transfer of the TM magneto-crystalline anisotropy (which then is larger than the RE anisotropy) to the RE sublattice; and (iii) J_{RT} determines the thermal stability of the 4f moments, hence the very strong temperature dependence of the RE anisotropy and also the critical temperature T_c (Buschow 1991).

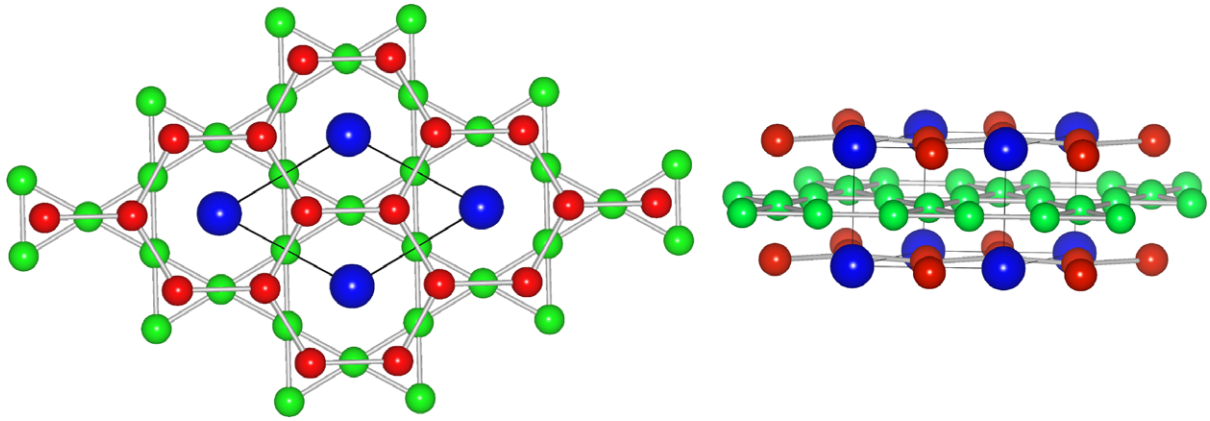

Figure 4. Illustration of the hexagonal $CaCu_5$ structure of $SmCo_5$ as an example of the $RETM_5$ phases; crystallographic sites Sm(1*a*) are shown in blue, Co(2*c*) in red and Co(3*g*) in green; the thin black lines indicate the unit cell.

3. Results and discussion

In the following, results are presented separately for the $RETM_5$, $RE_2TM_{14}B$ and RE_2TM_{17} structures which cover the best known RE:TM ratios of 1:5, 1:7 and 2:17.

3.1. Magnetic properties of $RETM_5$ phases

The simplest intermetallic phase $RETM_5$ considered here is chosen to illustrate the effect of substitutions on the magnetic properties. The compounds with the stoichiometry $RETM_5$ crystallize in the hexagonal $CaCu_5$-type structure shown in figure 4. For the calculation of the magnetic properties of this series we have applied experimental data for the atomic positions and lattice parameters of $SmCo_5$ (Steinbeck *et al* 2001). In this structure, the Sm atom occupies the crystallographic 1a site and Co atoms enter the 2c and 3g sites (here and in the following, the crystallographic sites are denoted as Wyckoff positions of the space groups (for details see the International Tables for Crystallography at http://it.iucr.org/ or the Bilbao Crystallography Server at http://www.cryst.ehu.es/). The $SmCo_5$ lattice parameters are kept constant (i.e. fixed length *a* and ratio *c*/*a*) during the HTS procedure for the entire series $RETM_5$.

On the TM sites in $REFe_5$ and $RECo_5$ compounds the effect of mutual substitutions of Co and Fe atoms on the two sublattices is investigated. The calculated total magnetic moments are shown in figure 5. The $RETM_5$ compounds with the light RE elements (Ce–Sm) possess higher magnetic moments than the ones with the heavy RE elements (Gd–Yb). (Note that Eu is a special case because it prefers a divalent ionic configuration over a trivalent one.) In the investigated series $RECo_5$, $RECo_3Fe_2$, $RECo_2Fe_3$ and $REFe_5$, maximal values for magnetic moments are found for RE = Pr, Nd.

The magnetic moments and exchange interactions in $Sm(Fe, Co)_5$ have been previously investigated theoretically (Liu and Altounian 2011). In our work we extend the treatment to the entire series of 4f-elements. The partial substitutions in $RECo_5$ with iron at crystallographic 2c or 3g positions have different effects on the magnetic properties in comparison to the pure $RECo_5$ and $REFe_5$ phases. Upon Co(2c) substitution with Fe, the total magnetic moment of $RECo_3Fe_2$ increases with values close to those of the only Fe-containing compounds

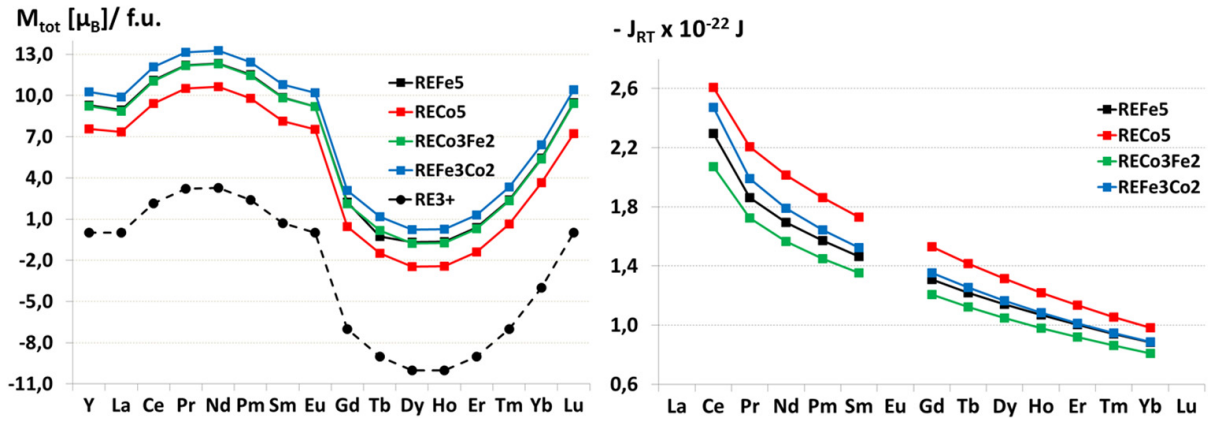

Figure 5. Total magnetic moments per formula unit (left) and exchange integrals (right) of the compounds from the $REFe_{5-x}Co_x$ series. The black circles and dashed line labeled RE^{3+} indicate the magnetic moments of free RE^{3+} ions.

$REFe_5$. The partial substitution of Co(3g) with Fe, leading to $REFe_3Co_2$, results in a further improvement of the magnetic properties. The total magnetic moments of $REFe_3Co_2$ even exceed the magnetic moments of the $REFe_5$ phases. This is because the local magnetic moment of Fe(3g) is highly reduced from about 2.4 μ_B in $RECo_3Fe_2$ to approximately 1.8 μ_B in $REFe_5$. A similar tendency has been found by Liu and Altounian (2011), their LSDA + U approach yielded a reduction of the Fe-magnetic moment from 2.5 to 2.0 μ_B. From the results for the local magnetic moments in $RECo_{5-x}Fe_x$ phases, we can conclude that simple linear interpolation assuming $\mu(\mathrm{Fe}) = 2.217\,\mu_B$ and $\mu(\mathrm{Co}) = 1.753\,\mu_B$ (Skomski 2008) to get an estimate for the magnitude of the magnetic moments of compounds is not generally applicable, since in some crystal structures some of these moments can be substantially quenched or enhanced. The better way to explore such tendencies is via systematic DFT computations.

The magnitude of the RE–TM exchange integrals J_{RT} for the $REFe_5$ and $RECo_5$ compounds decreases monotonically with the atomic number of the RE elements (see figure 5). Larger J_{RT} are found for $RECo_5$ in comparison to $REFe_5$. The Co(2c) substitutions with Fe lead to J_{RT} values smaller than those of $REFe_5$; the corresponding Co(3g) substitutions with Fe slightly increase the exchange-parameter values.

The dependence of the exchange integrals and magnetic moments on the unit cell size was investigated to check the applicability of the faster HTS procedure with lattice cell parameters kept fixed. For this purpose, the cell volume for each $RETM_5$ compound was optimized by minimization of the total energy with respect to the unit-cell volume with the TB-LMTO-ASA method. The magnetic properties are compared in figure 6.

The optimized lattice parameter decreases almost linearly from Ce to Lu (as expected according to the well-known trend of RE elements called 'lanthanide contraction'). The total change in the lattice parameter, however, amounts to only about 0.132 Å for the whole series of 4f-elements. As one can see in the right panel in figure 6, the change in the cell volume affects the total magnetic moments and exchange integrals very weakly, which gives a justification for the fast HTS procedure employed by keeping lattice parameters constant along the RE series.

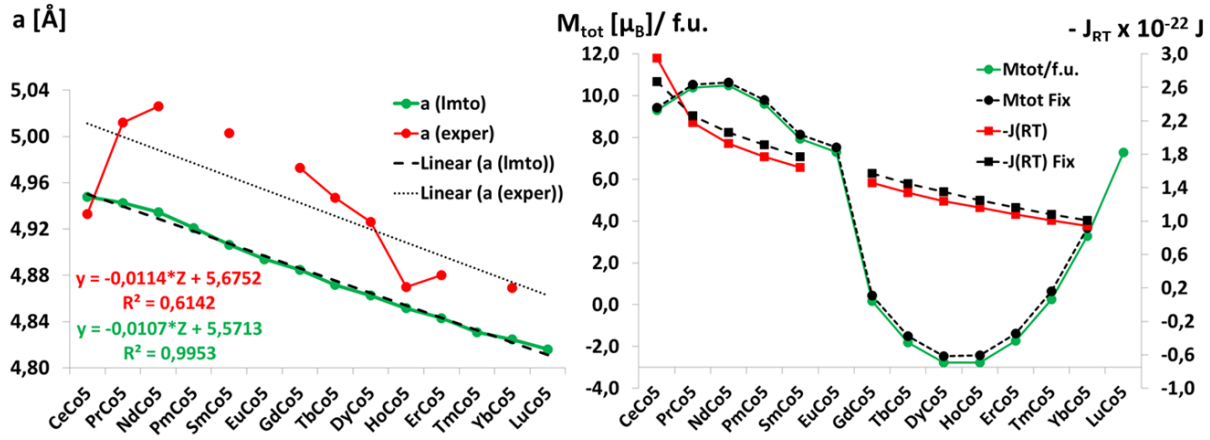

Figure 6. Change of the lattice parameters *a* (for fixed *c*/*a* ratio) with the atomic number of the RE element (left) and comparison of the magnetic properties for the optimized and fixed $RETM_5$ unit-cell volumes (right). In the left graph, the dashed and dotted black lines are linear fits to LMTO and experimental values (Grazulis *et al* 2009, Villars and Cenzual 2012/13) of lattice parameters.

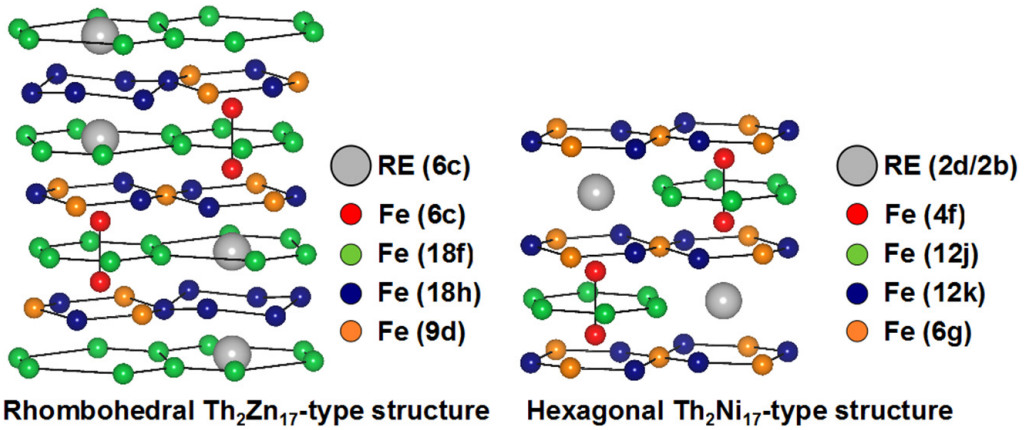

Figure 7. Crystal structures of the rhombohedral Th_2Zn_{17}-type (left) and hexagonal Th_2Ni_{17}-type (right) allotropes of RE_2Fe_{17} compounds.

3.2. Magnetic properties of RE_2TM_{17} compounds

The next challenge for the application of the developed HTS procedure is for intermetallic compound with several crystallographic sites for substitution, which extends substantially the possible variety of compositions. As an example we consider the RE_2TM_{17} phases which exist in two different allotropic forms—the rhombohedral Th_2Zn_{17}-type structure (left panel of figure 7) and the hexagonal Th_2Ni_{17}-type one (right panel of figure 7) (Rama Rao *et al* 1999). The rhombohedral structure is stable for the light RE elements (from Ce to Gd), whereas for the heavy RE elements (from Gd to Lu) the hexagonal one is more stable. The compounds with RE = Gd, Tb and Y exist in both forms depending on the conditions for synthesis (Buschow 1977, Rama Rao *et al* 1999). It has also been found for the RE_2TM_{17} compounds that some elements with small atomic radii (mainly hydrogen, carbon and nitrogen) can occupy IS sites

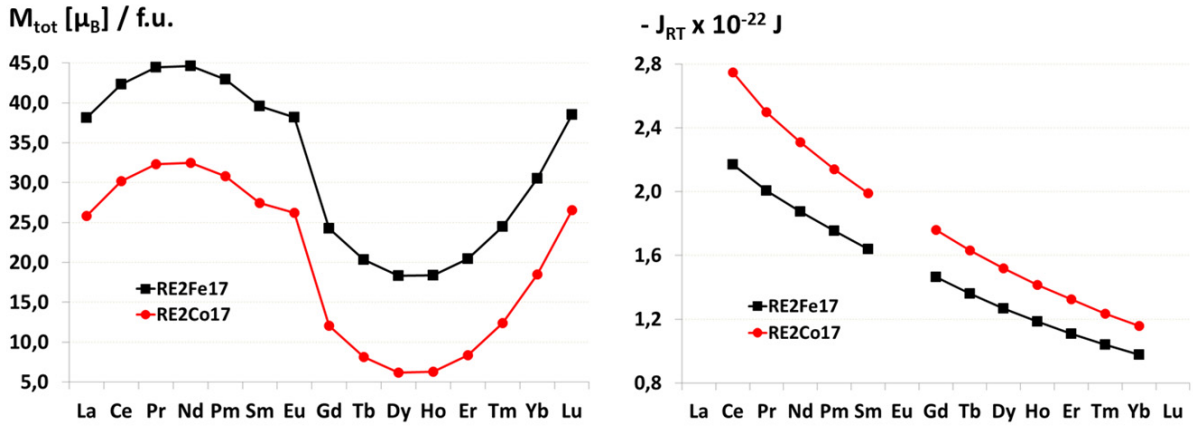

Figure 8. Computed total magnetic moments (left) and exchange integrals J_{RT} (right) for the pure iron and cobalt containing RE_2TM_{17} phases of Th_2Zn_{17}-type. The black lines represent the results for Fe, the red ones those for Co.

of rhombohedral or hexagonal structures thus causing lattice expansion and improving the magnetic properties of the compound (Isnard *et al* 1990, 1994, Zhong *et al* 1990, Ibberson *et al* 1991, Beuerle and Fähnle 1992, Sun *et al* 1992). The 2:17-type samarium-cobalt magnets possess excellent intrinsic magnetic properties such as high saturation magnetization, high anisotropy fields and very high Curie temperature; the latter being even superior to $Nd_2Fe_{14}B$ high-performance magnets (Schobinger *et al* 2002, Guo *et al* 2006). However, their high amount of the critical metal Co instead of Fe makes them very expensive.

In these compounds there are four crystallographic positions for the TM elements and either one position (for the rhombohedral structure) or two positions (for the hexagonal one) for the RE elements. In the *ab initio* screening procedure the atomic coordinates and lattice parameters for Nd_2Fe_{17} (Isnard *et al* 1990) are used for the Th_2Zn_{17}-type and those of Gd_2Fe_{17} (Knyazev *et al* 2006) for the Th_2Ni_{17}-type. Again as for the $RETM_5$ phases, the lattice constant was kept fixed to the value of Nd_2Fe_{17} for the entire series of RE elements and various TM substitutions when the magnetic properties were computed using the TB-LMTO-ASA method.

3.2.1. Magnetic properties of pure Fe- and Co-containing RE_2TM_{17} phases. Figure 8 shows the total magnetic moments M_{tot} and the exchange integrals J_{RT} for the pure Fe- and Co-containing phases of the entire series of RE elements. The results for the only Fe containing phases are shown in black, those for Co in red. One clearly sees that, like the $RETM_5$ phases (cf figure 5), the RE_2TM_{17} phases of Th_2Zn_{17}-type with light RE elements possess the larger total magnetic moments, with maxima at Pr and Nd. The Co-containing phases are characterized by lower magnetic moments, but their exchange integrals are larger. La, Eu and Lu are excluded from the computation of J_{RT} since, according to the Russell–Saunders coupling, their RE^{3+} ions have magnetic moments of approximately zero.

As can be seen from figure 8, the magnitude of the exchange integrals J_{RT} for both RE_2Fe_{17} and RE_2Co_{17} decreases with increasing atomic number of the RE element. A similar tendency was already observed by Belorizky *et al* (1987) for various classes of RE–TM intermetallics and related to the variation of the 4f–5d exchange interactions. These interactions are larger

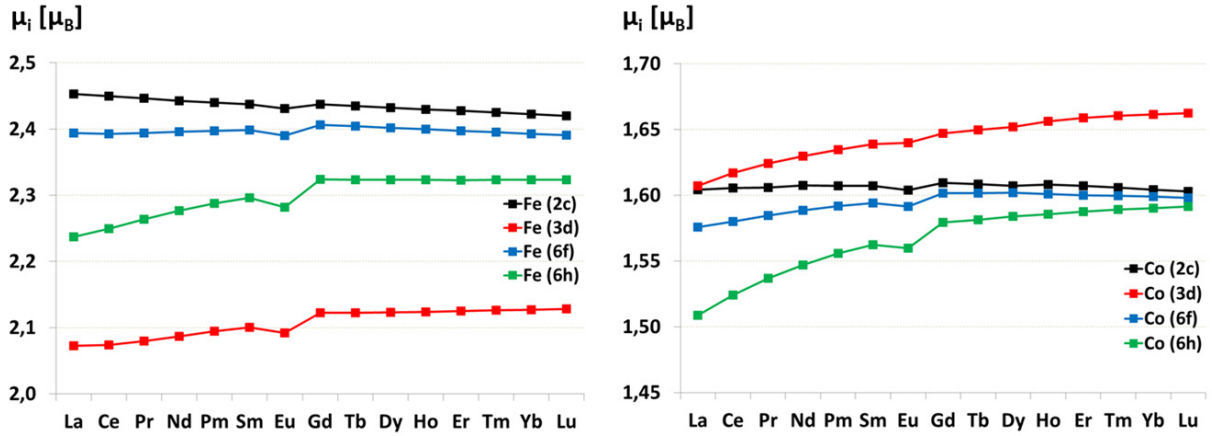

Figure 9. Local magnetic moments of Fe in RE_2Fe_{17} (left) and Co in RE_2Co_{17} (right) at the four different crystallographic positions in the rhombohedral Th_2Zn_{17}-type structure for the whole series of RE elements.

for the light RE since the difference between the spatial extent of the 4f and 5d electrons is reduced.

Additional insight into magnetic properties of the RE_2TM_{17} compounds can be obtained from the computed local magnetic moments. Figure 9 shows the changes in magnitude of the magnetic moments at the iron and cobalt sites of the TM-pure RE_2TM_{17} phases.

From figure 9 it is evident that the two TM elements Fe and Co interact quite differently with the RE sublattice, which leads to different ordering of the local magnetic moments at the four crystallographic 2c, 3d, 6f and 6h positions. For Fe the descending order of magnetic moments is μ(Fe-2c) > μ(Fe-6f) > μ(Fe-6h) > μ(Fe-3d) whereas for cobalt it is μ(Co-2c) > μ(Co-6f) > μ(Co-6h) > μ(Co-3d). This means that by exchanging Fe and Co at various crystallographic positions we can alter the magnetic properties in many ways.

3.2.2. Single and double substitutions of Fe by Co in Sm_2Fe_{17}. In the previous paragraph we described the magnetic properties of the purely Fe- and Co-containing RE_2TM_{17} phases. But in the RE_2TM_{17} phases, it is also possible to replace only some of the crystallographic TM positions with another TM element. To give an example, let us consider the Co and Mn substitution in Sm_2Fe_{17}, shown in figure 10. We chose this system as a representative case, since from all the RE_2TM_{17} compounds Sm_2Co_{17} is the most widely used hard magnetic phase. The results for Co substitutions are shown in blue, those for Mn in red. We can see that by adding small amounts of Co one just slightly lowers the total magnetic moments, thus approaching the moment of the purely Co-containing phase RE_2Co_{17}. Adding Mn leads to more pronounced lowering of the total magnetic moments; the total magnetic moments also approach that of the purely Mn-containing phase RE_2Mn_{17}. As concerns the exchange integrals J_{RT}, usually the single Co substitutions lead to a slight increase and the single Mn substitutions to a large reduction of the J_{RT}. The numerical values for the J_{RT} integrals of the substituted $Sm_2Fe_{17-x}Co_x$ compounds are in between those for Sm_2Fe_{17} and Sm_2Co_{17}.

It is straightforward to extend this replacement procedure to two or more crystallographic sites and thus to consider the effects of double, triple, quadruple, etc substitutions and to analyze

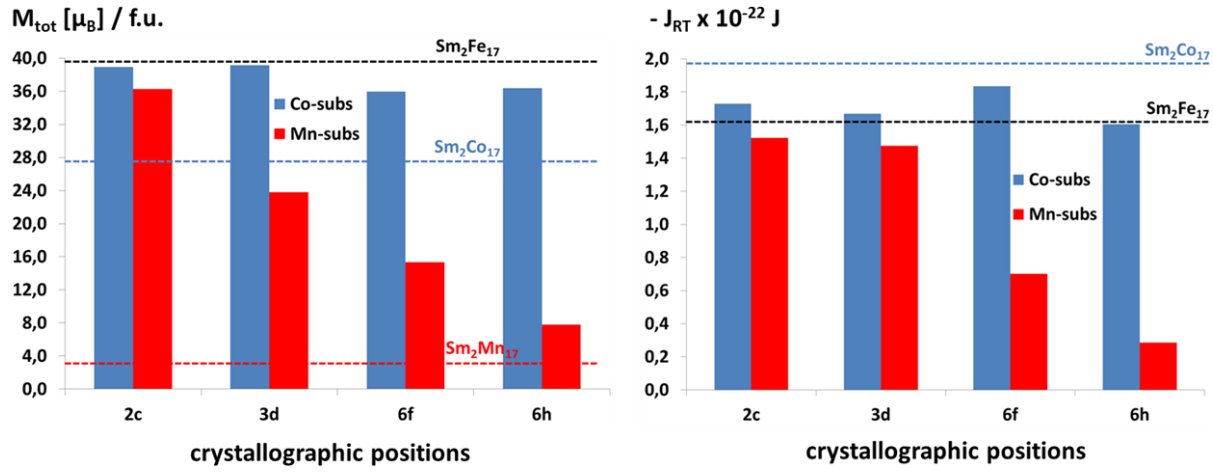

Figure 10. Computed values for the total magnetic moments M_{tot} (left) and exchange integrals J_{RT} (right) for the ternary phases $Sm_2Fe_{17-x}Co_x$ and $Sm_2Fe_{17-x}Mn_x$. The results for Co substitutions are shown in blue, those for Mn in red. The results for the binary systems are marked by dashed horizontal lines.

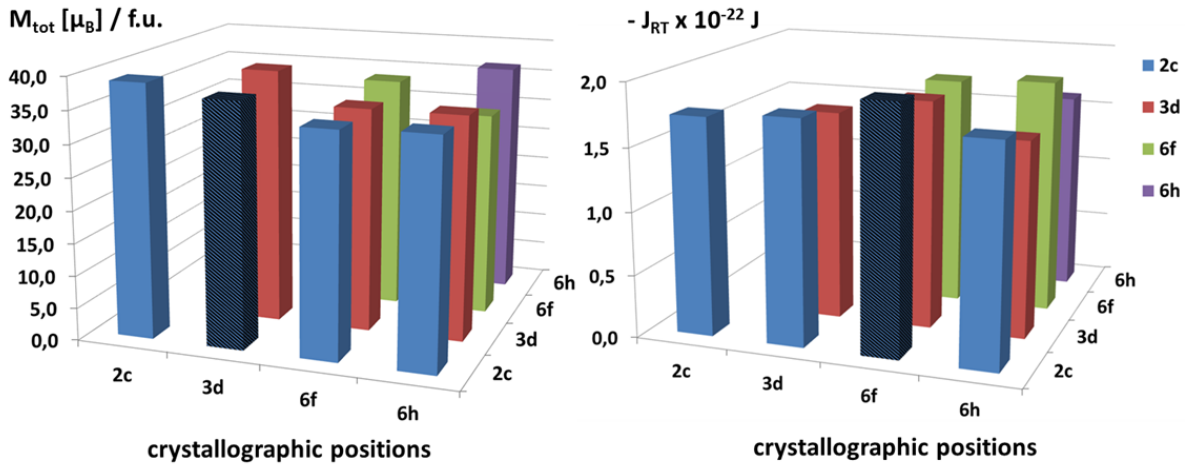

Figure 11. Two-dimensional charts representing the calculated total magnetic moments M_{tot} (left) and exchange integrals J_{RT} (right) in $Sm_2Fe_{17-x}Co_x$ for simultaneous substitutions of Fe by Co on two crystallographic positions. The diagonal elements correspond to single Co substitutions (cf figure 10) and are given here for comparison.

which ones more favorably lead to larger magnetic moments and exchange integrals. We have investigated, e.g., the effect of cobalt substitutions on two crystallographic positions, the results are summarized in figure 11 below.

Since Co has a lower magnetic moment per atom than Fe ($\mu_{\mathrm{Co}} = 1.753\,\mu_{\mathrm{B}}$ versus $\mu_{\mathrm{Fe}} = 2.217\,\mu_{\mathrm{B}}$ for pure Co and Fe metals, respectively (Skomski 2008)), it is likely that the double Co substitution may lead to a further decrease of the total magnetic moments. However, a maximum of the total magnetic moments is achieved by double substitution at the pair of crystallographic

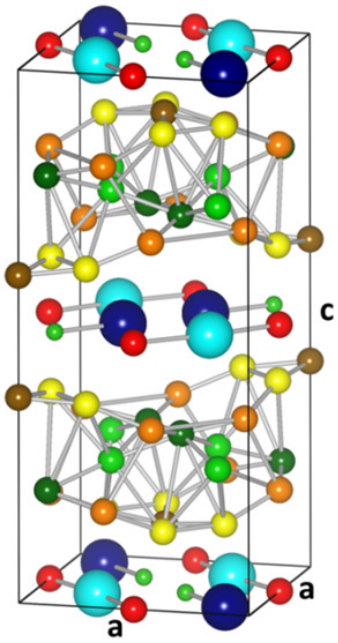

Atom	x	y	z
Nd(4f)	0.268	0.268	0.0
Nd(4g)	0.140	-0.140	0.0
Fe($16k_1$)	0.223	0.567	0.127
Fe($16k_2$)	0.037	0.360	0.176
Fe($8j_1$)	0.098	0.098	0.204
Fe($8j_2$)	0.317	0.317	0.246
Fe(4e)	0.5	0.5	0.114
Fe(4c)	0.0	0.5	0.0
B(4g)	0.371	-0.371	0.0

Figure 12. Unit cell of the $Nd_2Fe_{14}B$ compound according to Herbst. The experimental lattice parameters are $a = 0.88$ nm, $c = 1.22$ nm. The c-axis was manually elongated to emphasize the puckering of iron layers as in Fähnle *et al* (1993).

2c and 3d positions, which corresponds to the atomic composition $Sm_2Fe_{12}Co_5$. As concerns the exchange parameters, a maximum value for J_{RT} is obtained for the 2c–6f double substitutions, i.e. for $Sm_2Fe_9Co_8$. This finding again supports the above statement that linear correlation of magnetic properties with chemical compositions is not generally valid and explicit DFT computation is better for analyzing and predicting magnetic properties.

3.3. Magnetic properties of Nd–Fe–B magnets and the $RE_2TM_{14}B$ series

Since the discovery of the hard ferromagnetic compound $Nd_2Fe_{14}B$, for its development to the strongest available permanent magnet it has been a challenge to further improve its magnetic properties by compositional variations of the $RE_2Fe_{14}B$ system. This may be achieved for instance by substituting Nd with another RE element, replacing totally or in part Fe by other TM elements like Co or Ni, or by exchanging B with other light IS (interstitial) atoms such as H, C and N. Because the combinatorial variety of possible intermetallic $RE_2TM_{14}IS$ phases increases very rapidly, it is essential to obtain guidelines from theory for a systematic search for new materials.

The exact stoichiometry and crystal structure of $Nd_2Fe_{14}B$ were determined independently and simultaneously by three research groups in 1984 (Givord *et al* 1984a, 1984b, Herbst *et al* 1984, Shoemaker *et al* 1984). Figure 12 displays the $Nd_2Fe_{14}B$ unit cell. The crystal structure has tetragonal symmetry (space group $P4z/mnm$), and each unit cell contains four formula units, i.e. 68 atoms. There are six crystallographically distinct TM sites ($16k_1$, $16k_2$, $8j_1$, $8j_2$, $4c$ and $4e$), two different RE positions (4f and 4g) and one IS site ($4g$).

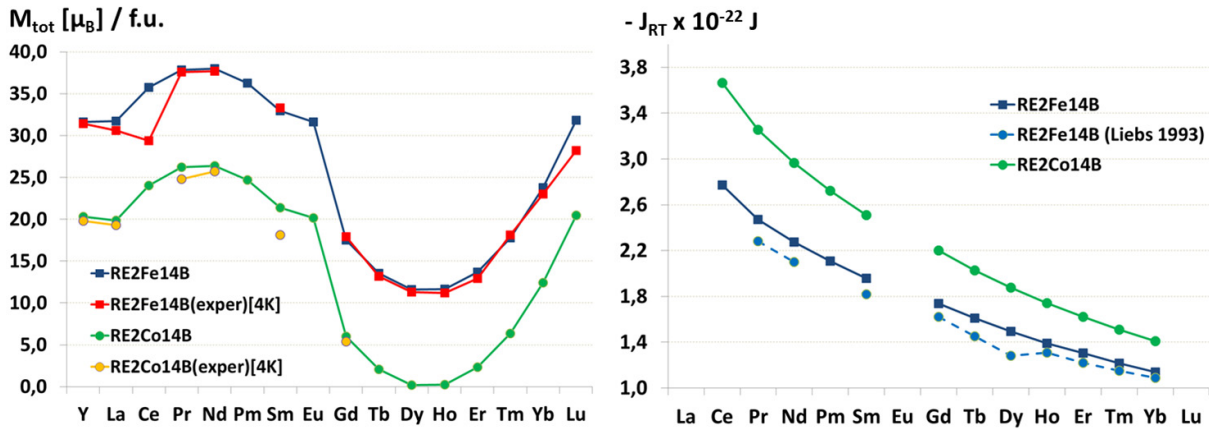

Figure 13. Computed values for the total magnetic moments M_{tot} (left) and exchange integrals J_{RT} (right) in $RE_2Fe_{14}B$; for comparison, experimental M_{tot} data in the left graph are from Herbst (1991), theoretical J_{RT} data in the right graph from Liebs *et al* (1993).

Analogies with the hexagonal $CaCu_5$ structure characterizing the permanent magnet $SmCo_5$ and a variety of other RE–TM phases can be found in Herbst (1991) and references given therein.

In the *ab initio* screening of the magnetic properties in $RE_2TM_{14}B$ compounds we used the experimental atomic positions and lattice parameters from Croat *et al* (1984). The results are presented in figure 13 and compared with those from previous theoretical (Liebs *et al* 1993) and experimental investigations (Herbst 1991).

The computed results from the HTS procedure for the total magnetic moments show very good agreement with the experimental values for both $RE_2Fe_{14}B$ and $RE_2Co_{14}B$. The largest discrepancy for the total magnetic moments is found for $Ce_2Fe_{14}B$ and $Sm_2Co_{14}B$, respectively. This difference can be attributed to the tendency of Ce and Sm to form mixed valence intermetallics, which could lead to a deviation from the RE^{3+} configurations used in the calculations. The calculated J_{RT} integrals also follow the same tendency as those found in the paper of Fähnle *et al* (1993) and Liebs *et al* (1993). The good agreement with experiment indicates again that one can compute reliable estimates for the magnetic moments with the fast TB-LMTO-ASA method.

4. Accurate density functional theory calculations with no potential-shape approximation

The results from the fast *ab initio* screening procedure with the TB-LMTO-ASA method reveal most of the features in the magnetic properties of the investigated RE–TM intermetallic phases. However, the examples provided in this paper are for well-known RE–TM phases. If we want to go beyond this and predict new phases as candidates for permanent magnetic materials we have to check the accuracy of the TB-LMTO-ASA method with DFT methods beyond the potential-shape restricting atomic-sphere approximation and to be able to compute the Curie temperature (T_c) and the magnetocrystalline anisotropy constant (K_1).

We have investigated some selected systems by performing spin-polarized calculations using VASP (versions 4 and 5) (Kresse 1993, Kresse and Hafner 1993, Kresse and Furthmüller

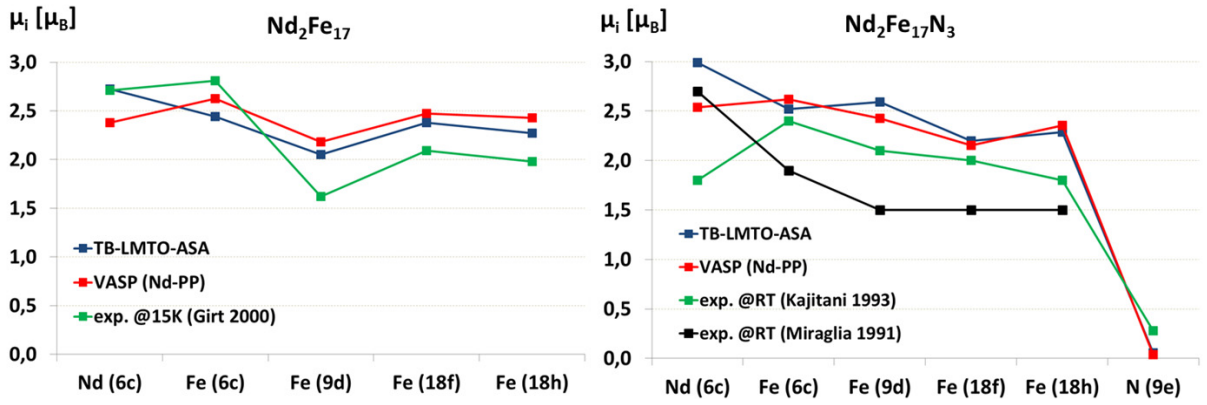

Figure 14. Comparison of the local magnetic moments for Nd_2Fe_{17} (left) and $Nd_2Fe_{17}N_3$ (right) calculated with TB-LMTO-ASA and VASP programs with reported experimental values (Miraglia *et al* 1991, Kajitani *et al* 1993, Girt *et al* 2000).

1996a,1996b). Starting from experimental values, with VASP the lattice parameters and atomic positions are fully relaxed, and then the magnetic properties are calculated. In the LSDA calculations projector augmented wave potentials provided in VASP were used. After checking for convergence of the total energy differences for several systems, an energy cutoff of 400 eV for the plane-wave basis was selected for all the calculations. The *k*-points distribution was checked for convergence as well (e.g. for $Nd_2Fe_{14}B$ system with 68 atoms in the unit cell a $5 \times 5 \times 4$ Monkhorst-pack grid was used). Convergence criteria for the structure relaxation were set to 10^{-5} eV and 0.01 eV $Å^{-1}$ for the energies and forces, respectively.

As concerns the accuracy of the TB-LMTO-ASA method for predicting the magnetic moments and the exchange interactions of the RE–TM intermetallics, we have compared some results of this method with those obtained by the full-potential LSDA calculations with VASP. The results for the hexagonal Nd_2Fe_{17} and $Nd_2Fe_{17}N_3$ compounds are summarized in figure 14.

There is in general very good agreement between the results computed with both the fast DFT method and the accurate one, and with the experimental magnetic moments for both Nd_2Fe_{17} and $Nd_2Fe_{17}N_3$ phases, as can be seen from figure 14. The addition of nitrogen is expected to lead to a dilation of the lattice and thus to higher magnetic moments, which is well reproduced by both VASP and TB-LMTO-ASA.

5. Estimating the magnetocrystalline anisotropy energy with Vienna *ab initio* simulation package

The MAE is determined with VASP by doing a set of calculations starting with the self-consistent DFT density and Kohn–Sham wave functions obtained with the magnetization oriented in the *z*-direction (easy axis [001]) and gradually changing the direction of the spin quantization axis from this direction to the [100] or [110] direction, respectively, without recalculation of the wave functions. Total energies per unit cell are calculated for a series of orientations of the quantization axis, and then a polynomial function in the rotation angles with respect to the *z*-axis is fitted to the total-energy data. The form of the polynomial function depends on the symmetry of the crystal. For $Nd_2Fe_{14}B$ the MAE is expressed

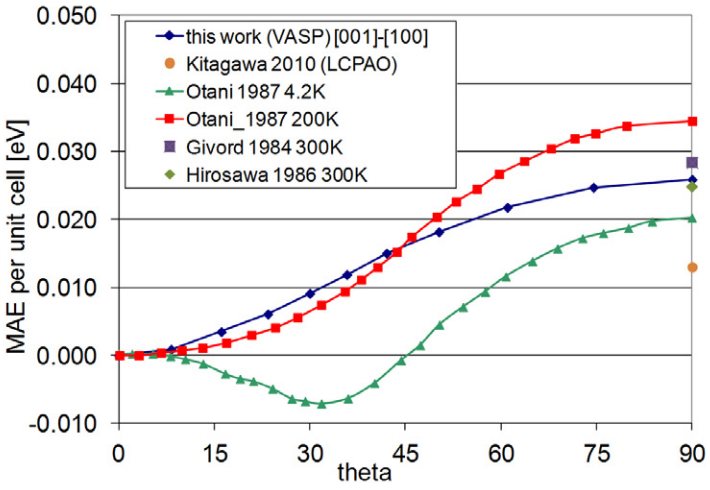

Figure 15. The dependence of the MAE per unit cell on the orientation of the quantization axis with respect to the tetragonal c-axis for $Nd_2Fe_{14}B$. The blue line indicates the result of our VASP calculation. The green and red lines are from measurements under and above the reorientation transition temperature of the crystal, respectively. These data are reported in Otani *et al* (1987). Additional experimental (Givord *et al* 1984a, 1984b, Hirosawa *et al* 1986) and calculated data (Kitagawa and Asari 2010) for the MAE for a change of the magnetization direction from [001] to [100] are marked by symbols at $\theta = 90^\circ$.

by (Givord *et al* 1984a, 1984b)

$$E_a = K_1 \sin^2\theta + K_2 \sin^4\theta + K_3 \sin^4\theta \cos^4\theta, \tag{2}$$

where K_1, K_2, K_3 are the anisotropy constants, θ and φ are the angles of magnetization with respect to [001] and [100], respectively.

Note that for $Nd_2Fe_{14}B$ at a transition temperature of 135 K a reorientation of the magnetic easy axis from a low-temperature orientation of $\theta = 32.3^\circ$ inclined to [001] to an orientation parallel to the [001] direction takes place (Otani *et al* 1987, Wolfers *et al* 1996). This means that the experimental MAE curves at temperatures below 135 K have a minimum away from the [001] direction (figure 15, green curve at 4.2 K), and only for temperatures above this transition temperature does the easy axis coincide with the [001] direction (figure 15, red curve at 200 K). Thus, the theoretical MAE curves (and the derived K_1 and K_2 constants) calculated with the procedure implemented in VASP (figure 15, blue curve), where the easy axis is set in the [001] direction, are to be compared with the experimental data above the transition temperature.

The values for the anisotropy constants K_1 and K_2 obtained from the fits of equation (3) to the curves for small angles in the vicinity of the easy axis [001] are given in table 1 for different changes in the magnetization direction ([001]–[100] and [001]–[110]). They are compared with experimental data found in the literature for two temperature ranges, and with a value estimated from theoretical crystal-field parameters A_2^0 calculated with a full-potential linear-muffin-tin-orbital method (FP-LMTO) (Hummler and Fähnle 1996).

For $Nd_2Fe_{14}B$ the differences between our calculated values and the experimental values around room temperature are within the spread between the different experimental results. Our calculated values for K_1 have less than 2% difference to the one obtained from the calculated

Table 1. Magnetocrystalline anisotropy constants calculated with VASP for $RE_2Fe_{14}B$ compounds with RE = Ce, Pr and Nd.

Compound	Anisotropy constant ($MJ\,m^{-3}$)	Calculated [001]–[100]	Calculated [001]–[110]	Experimental values 4.2 K		270–300 K		Calculated FP-LMTO-LSDA
$Ce_2Fe_{14}B$	K_1	2.10	2.07	1.65[a]	–	1.44[a]	–	
$Pr_2Fe_{14}B$	K_1	4.85	4.89	2.35[a]	–	5.5[a]	–	
$Nd_2Fe_{14}B$	K_1	6.18	6.26	−6.5[b]	−8.59[c]	3.7[b]	5.15[c]	6.08[d]
B	K_2	2.06	2.09	14[b]	23.3[c]	1.5[b]	0.69[c]	–

Corresponding experimental values are taken from:
[a] Sagawa (1987) at 300 K.
[b] Otani *et al* (1987) at 4.2 K.
[c] Pastushenkov *et al* (2005) at 270 K.
[d] This theoretical value is estimated from theoretical crystal-field parameters A_2^0 for the two Nd sites in $Nd_2Fe_{14}B$ calculated by Hummler and Fähnle (1996).

A_2^0 values from Hummler and Fähnle (1996). Similarly good agreement holds between our calculated values for K_1 for $Pr_2Fe_{14}B$ and $Ce_2Fe_{14}B$ and the corresponding experimental ones reported at room temperature. Moreover, our calculated values for the total MAE obtained by changing the magnetization axis completely from [001] to [100] almost coincide with the values reported by Givord *et al* (1984a, 1984b) and Hirosawa *et al* (1986), and they are in better agreement with the experimental data than other calculated values using linear combination of pseudo-atomic-orbitals within the LSDA + U approximation (Kitagawa and Asari 2010).

We conclude that the VASP method allows to calculate values for anisotropy constants of hard-magnetic RE–TM phases that reproduce in general the typical behavior of complex magnetic materials, and that it has predictive power for the evaluation of the MAE by complete tilting ($\theta = 90^\circ$) of the magnetization direction.

6. Estimate of the Curie temperature (T_c)

Another major challenge in the computational search for new candidates for permanent magnetic materials is to get a reasonable estimate of the Curie temperature (T_c), which is essentially determined by the interatomic exchange interactions. The two-sublattice model considered above provides a good approach to determine the exchange interaction between RE and TM sublattices. However, for T_C it is the exchange interaction between the TM atoms which is more relevant, and therefore the distance-dependent TM–TM exchange integrals between TM atoms on different sublattices have to be calculated. The problem of calculating the magnetic TM–TM exchange interactions and determining T_C therewith for RE–TM phases was addressed recently by Lukoyanov *et al* for Gd_2Fe_{17} in its rhombohedral and hexagonal lattice structures (Lukoyanov *et al* 2009). They used the calculated values of exchange parameters for the first- and second-neighbor coordination spheres in both structure types and estimated T_C on the basis of Weiss' mean-field theory.

Alternatively to the mean-field approach, T_C can be determined as well from the exchange parameters by means of numerical finite-temperature Monte Carlo simulations. In this work,

we chose this procedure. The computation of the pairwise TM–TM exchange interactions, J_{ij}, needed therefore was done with the method proposed by Liechtenstein *et al* (1987). This method provides a rigorous expression for the pair exchange parameters of the classical Heisenberg model

$$E = -\sum_{\substack{i,j \\ i \neq j}} J_{ij} s_i s_j \tag{3}$$

applied to crystals, and the parameters are obtained by LSDA calculations. The total magnetic state of all atoms is described by the set of normalized spin vectors $\{s_i\}$ (the subscript i is the atom index). In order to determine the exchange parameters J_{ij} one must calculate the total energy for small deviations of a single magnetic moment and a pair of magnetic moments from the ferromagnetic ground-state configuration. This results in energy E_i for a spin configuration s^i and energy E_{ij} for a spin-pair configuration s^{ij}, where the superscript indicates the tilted spins. The exchange interaction J_{ij} is calculated from

$$E_{ij} - E_i - E_j + E_{\mathrm{ref}} = -2J_{ij}(s_i^{ij} s_j^{ij} - s_i^i s_j^i - s_i^j s_j^j + s_i^{\mathrm{ref}} s_j^{\mathrm{ref}}). \tag{4}$$

For small periodic unit cells one has to divide the resulting J_{ij} by the number of occurrences of the interaction due to periodic images of spins. This approach, however, is valid for $T = 0\,\mathrm{K}$ only. To consider finite temperatures with DFT one needed to know the temperature dependence of the LSDA exchange-correlation functional which is not known yet (Liechtenstein *et al* 1987).

In order to reduce the number of necessary DFT calculations of tilted spin states for a given set of exchange interactions, the symmetry of the crystal structure was exploited to determine a pairwise non-symmetric subset of interactions. Where necessary the space group of the crystal structure was detected (Hannemann *et al* 1988). The energies of the tilted spin states were calculated with VASP. Since the local magnetic moments are integrals of the magnetization in a site centered sphere, they cannot be set directly and the spin orientations were constrained with a penalty contribution to the total energy expression.

A serial Monte Carlo program for a general crystal structure was developed using the Metropolis *et al* (1953), Swendsen and Wang (1987) and Wolff (1989) methods for the spin models of Ising (1925) and Heisenberg (1928). In contrast to the Metropolis method the latter algorithms do not flip single spins but a cluster of spins, which were calculated with the Hoshen–Kopelman algorithm (Hoshen *et al* 1979). The Curie temperature was determined as the intersection of the fourth-order cumulant of magnetization–temperature curves for different sized systems (Shan-Ho and Salinas 1998).

The exchange interactions for bcc Fe have been calculated for interatomic distances up to 8.2 Å, i.e. the 12th nearest neighborhood, and resulted in a Curie temperature of 1100 K. This is in good agreement with the experimental value of 1043 K (Yousuf *et al* 1986). For $SmCo_5$ with interactions up to only 3.2 Å the resulting calculated T_C value of 2500 K does not yet reproduce well the experimental Curie temperature of 985 K (Tie-Song *et al* 1991). Therefore further neighborhoods of interactions need to be taken into account. This is still work in progress.

7. Thermodynamic stability of rare-earth–transition-metal phases

The theoretical characterization of new phases with favorable magnetic properties is only the first step for the real discovery of a new magnetic material. Before experimental work for the

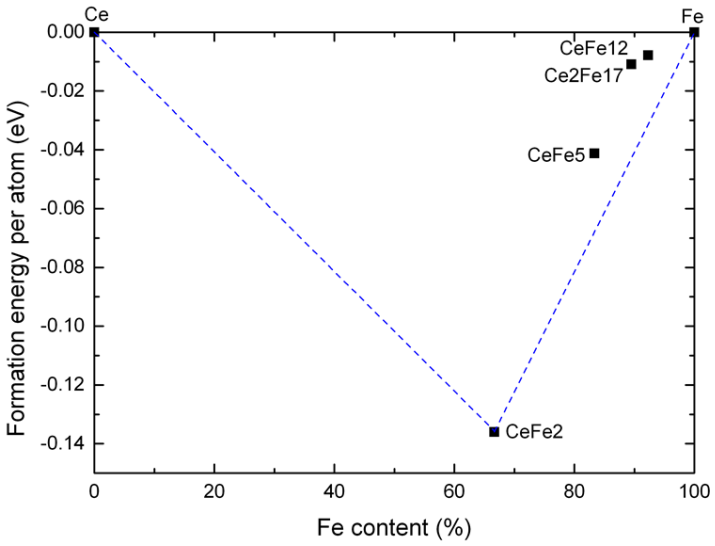

Figure 16. Calculated formation energies of the $CeFe_x$ phases as a function of the iron content. Higher negative values imply more stable phases. The resulting convex hull is drawn with dashed lines.

synthesis of a promising candidate begins, modeling should give some confidence as well about the expectable thermodynamic stability of the new material. In the following we give only a concise outlook on the current extension of our HTS procedure in this direction.

A first evaluation of the stability can be done by comparing the formation energies calculated by DFT methods like VASP. This procedure and its possibilities are illustrated by discussing the thermodynamic stability in the Ce–Fe system. Phases based on Ce and Fe show potential for alternative hard magnetic materials, since both these RE and TM elements are abundant and comparatively cheap. In addition, the magnetic properties of Ce_xFe_y phases calculated with TB-LMTO-ASA (not shown here) are also in an acceptable range.

In the binary phase diagram of the Ce–Fe system (Okamoto 2008) there are only stable phases identified for four compositions: Ce, $CeFe_2$, Ce_2Fe_{17} and Fe. There are additional reports about the synthesis of $CeFe_5$ in the literature (Jepson and Duwez 1955). We calculated the formation energies of the known binary phases with respect to the pure metallic elemental phases of fcc Ce and bcc Fe. The results for the formation energy for the different phases including $CeFe_{12}$ are shown in figure 16. None of the phases $CeFe_5$, $CeFe_{12}$ and Ce_2Fe_{17} seem to be stable in the sense that they are not part of the stability convex hull of the system (Hildebrandt and Glasser 1994). Phases with more than 66.6% content of Fe would decompose into $CeFe_2$ and Fe. Particularly for Ce_2Fe_{17} this result is a consequence of the neglect of the contribution of temperature-dependent terms to the total energy of the material. Actually, preliminary calculations including vibrational-energy contributions for the binary Ce–Fe system predict stability for Ce_2Fe_{17} starting at a temperature of about 600 K, where this phase becomes a vertex of the convex hull (in the experimental phase diagram this change occurs at about 1200 K).

As a strategy for the stabilization of $CeFe_{12}$, which has the most favorable RE:TM proportion within the binary phases, some of the Fe atoms are substituted by other elements. The existence of known stable phases of related ternary phases $RETM_{10}Si_2$, like $YFe_{10}Si_2$ and

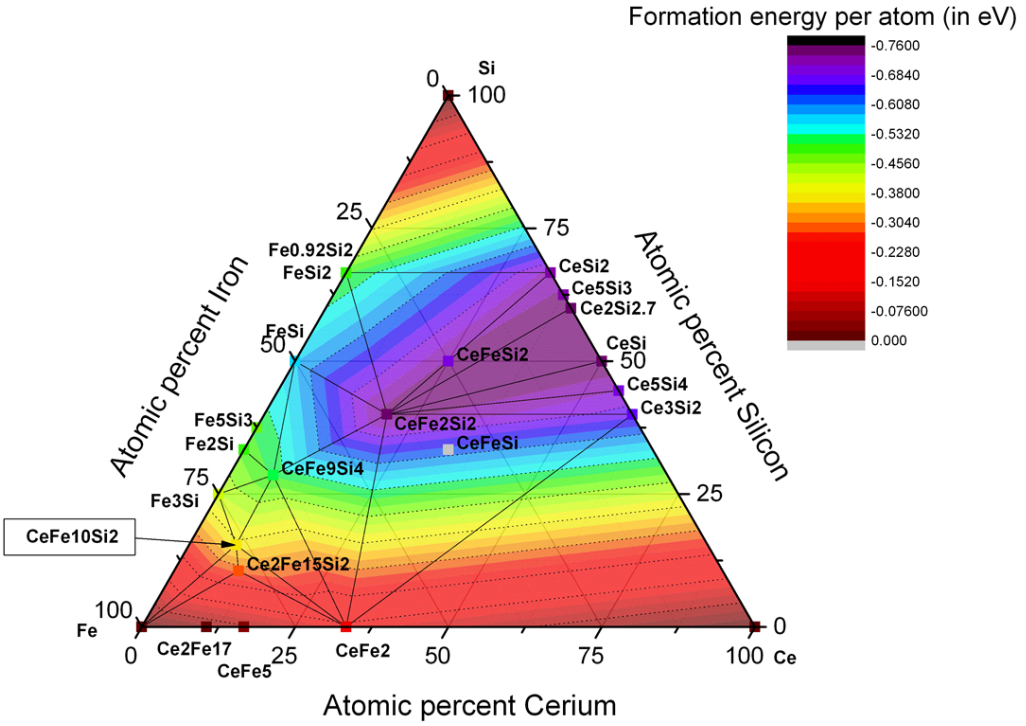

Figure 17. Calculated phase diagram of the Ce–Fe–Si system based on formation energies calculated with VASP. The color scale gives the formation energies in eV per atom. Black lines connect the convex hull vertices.

$GdFe_{10}Si_2$ (Mooij and Buschow 1988), points to the possibility of trying the stabilization with a double substitution of Fe by Si. This substitution results in a formation energy of −0.37 eV per atom, far lower than the formation energy of $CeFe_2$ in the binary Ce–Fe system, which makes the ternary phase apparently more stable than the binary one. Unfortunately this potentially new ternary phase $CeFe_{10}Si_2$ has also to compete with all other known binary and ternary phases of the ternary Ce–Fe–Si configuration space.

Finding in the literature all known mixed phases for a given combination of several elements is a cumbersome task. To make it easier, a screening tool was designed to screen the most common crystallographic data bases, namely Inorganic Crystal Structure Database (Bergerhoff and Brown 1987), Crystallography Open Database (Grazulis *et al* 2009) and Pearson's Crystal Data (Villars and Cenzual 2012/13): given the list of elements of interest, the software finds all binary, ternary and more-components mixed phases, automatically eliminates duplicate entries and lists the atomic compositions, crystal structures and the literature citations. In a future advanced version this HTS tool will also be capable of creating the input files for a chosen DFT code to run the calculation of the formation energies.

Figure 17 shows the result from our VASP calculations for the Ce–Fe–Si system, including the interesting new candidate $CeFe_{10}Si_2$. In the framework of the approximate DFT total energies, the proposed phase is part of the convex hull of the ternary system and in this way also predicted to be stable. Yet more accurate DFT calculations are needed to confirm this result since the new phase is located in the vicinity of experimentally reported phases of the composition

$Ce_2Fe_{(15.0–16.5)}Si_{(2–0.5)}$ and $CeFe_{(9.5–8)}Si_{(3.5–5)}$. These two substitutional phases are represented in our calculation by single compositions $CeFe_9Si_4$ and $Ce_2Fe_{15}Si_2$, and have probably a high entropic contribution to their total energy.

Further improvement is needed in this procedure to include in an automatized way more exact estimations for the total energies of the involved systems, taking into account further terms like vibrational free energies and configurational entropies for phases with substitutional elements.

8. Summary and outlook

In this paper we presented an efficient and robust HTS methodology for the systematic computation of the intrinsic magnetic properties of various intermetallic RE–TM compounds by using fast and reliable first-principle methods based on DFT. The HTS procedure was tested for a selection of known hard magnetic phases such as $RETM_5$, RE_2TM_{17} and $RE_2TM_{14}B$. The effects of different RE and TM substitutions on the total magnetic moments and exchange integrals were thoroughly investigated with the fast TB-LMTO-ASA method for each intermetallic phase. It was shown that for the selected as promising hard magnetic materials it is possible to compute the Curie temperature (T_c) and magnetocrystalline anisotropy constants (K_1) with more accurate DFT calculations using VASP and thus to determine the main prerequisites for practically useful permanent magnetic materials. The task of predicting structural stability of the RE–TM phases was also addressed using VASP. Our described HTS approach is able to determine the main guiding principles in the selection of proper crystal structures and atomic compositions, which can lead to new candidates for hard magnetic phases. In a next step, we are going to apply the proposed HTS procedure to predict the relative stability of the RE–TM phases and screen more general classes of topologically close-packed phases for promising candidates of permanent magnetic materials.

Acknowledgments

This work was supported by the Cooperative Project ‘Suche nach neuen hartmagnetischen Phasen mit hoher Energiedichte (REleaMag)’ (grant number 03X4626A) funded by the German Federal Ministry of Education and Research (BMBF). We are grateful to Professor Olivier Isnard for critical reading of the manuscript. Some of the authors (AM, LK, AG, TS and TE) would like to express their sincere thanks to the crew of Center for Computational Materials Science of the Institute for Materials Research, Tohoku University for their continuous support of the SR16000 supercomputing facilities. We especially want to thank Professor Yoshiyuki Kawazoe (Tohoku University, Japan) for many stimulating and highly valuable discussions.

References

Alonso E *et al* 2012 *Environ. Sci. Technol.* **46** 3406–14
Andersen O K 1975 *Phys. Rev.* B **12** 3060
Andersen O K and Jepsen O 1984 *Phys. Rev. Lett.* **53** 2571
Belorizky E *et al* 1987 *J. Appl. Phys.* **61** 3971–3
Bergerhoff G and Brown I D 1987 *Crystallographic Databases* ed F H Allen *et al* (Chester: International Union of Crystallography)

Beuerle T and Fähnle M 1992 *Phys. Status Solidi* b **174** 257–72
Blundell S 2001 *Magnetism in Condensed Matter* (Oxford Master Series in Physics) (Oxford: Oxford University Press) pp 90–3
Brooks M S S, Nordström L and Johansson B 1991a *J. Phys.: Condens. Matter* **2** 2357
Brooks M S S, Nordström L and Johansson B 1991b *J. Phys.: Condens. Matter* **3** 3393
Burzo E, Chelkowski A and Kirchmayr H 1990 Compounds between rare earth elements and 3d, 4d, or 5d *Landolt–Börnstein, Vol. 19, 'Magnetic Properties of Materials', Part 19d2* ed H P J Wijn (Berlin: Springer) pp 1–405
Buschow K H J 1977 *Rep. Prog. Phys.* **40** 1179–256
Buschow K H J 1991 *Rep. Prog. Phys.* **54** 1123
Coey J M D 1996 *Rare-Earth Permanent Magnets* (Oxford: Clarendon)
Coey J M D 2011 *IEEE Trans. Magn.* **47** 4671
Coey J M D 2012 *Scr. Mater.* **67** 524–9
Croat J J, Herbst J F, Lee R W and Pinkerton F E 1984 *J. Appl. Phys.* **55** 2083
Curtarolo S *et al* 2013 *Nature Mater.* **12** 191–201
Fähnle M, Hummler K, Liebs M and Beuerle T 1993 *Appl. Phys.* A **57** 67–76
Gasi T *et al* 2013 *Phys. Rev.* B **87** 064401
Gilleßen M and Dronkowski R 2009 *J. Comput. Chem.* **30** 1290–9
Gilleßen M and Dronkowski R 2010 *J. Comput. Chem.* **31** 612–9
Girt E *et al* 2000 *J. Appl. Phys.* **87** 5323–5
Givord D, Li H and Moreau J 1984a *Solid State Commun.* **50** 497
Givord D, Li H S and Perrier de la Bâthie R 1984b *Solid State Commun.* **51** 857–60
Grazulis S *et al* 2009 Crystallography open database—an open-access collection of crystal structures *J. Appl. Crystallogr.* **42** 726–9
Guo Z H, Pan W and Li W 2006 *J. Magn. Magn. Mater.* **303** e396–401
Gutfleisch O *et al* 2011 *Adv. Mater.* **23** 821–42
Hannemann A, Hundt R, Schoen J C and Jansen M 1988 *J. Appl. Crystallogr.* **31** 922–8
Heisenberg W 1928 *Z. Phys.* **49** 619–36
Herbst J F 1991 *Rev. Mod. Phys.* **63** 819
Herbst J F, Croat J J, Pinkerton F E and Yelon W B 1984 *Phys. Rev.* B **29** 4176–8
Hildebrandt D and Glasser D 1994 *Chem. Eng. J. Biochem. Eng. J.* **54** 187–97
Hirosawa S *et al* 1986 *J. Appl. Phys.* **59** 873
Hoshen J, Klymko P and Kopelman R 1979 *J. Stat. Phys.* **21** 583–600
Hummler K and Fähnle M 1996 *Phys. Rev.* B **53** 3290
Ibberson R M, Moze O, Jacobs T H and Buschow K H J 1991 *J. Phys.: Condens. Matter* **3** 1219–26
Ising E 1925 *Z. Phys.* **31** 253–8
Isnard O *et al* 1990 *J. Less-Common Metals* **162** 273–84
Isnard O *et al* 1994 *J. Magn. Magn. Mater.* **137** 151–6
Jepson J O and Duwez P E 1955 *Trans. Am. Soc. Met.* **47** 543–53
Kajitani T *et al* 1993 *J. Appl. Phys.* **73** 6032–4
Kiss J, Chadov S, Fecher G H and Felser C 2013 *Phys. Rev.* B **87** 224403
Kitagawa I and Asari Y 2010 *Phys. Rev.* B **81** 214408
Knyazev Y V *et al* 2006 *Phys. Rev.* B **73** 094410
Kramers M J, McCallum R W, Anderson I A and Constantinides S 2012 *JOM* **64** 752
Kresse G 1993 *PhD Thesis* Technische Universität Wien, Vienna, Austria
Kresse G and Furthmüller J 1996a *Comput. Mater. Sci.* **6** 15
Kresse G and Furthmüller J 1996b *Phys. Rev.* B **54** 11169
Kresse G and Hafner J 1993 *Phys. Rev.* B **47** RC558
Kresse G and Joubert D 1999 *Phys. Rev.* B **59** 1758

Liebs M 1992 *MSc Thesis* University of Stuttgart, Stuttgart, Germany
Liebs M, Hummler K and Fähnle M 1993 *J. Magn. Magn. Mater.* **124** 239–42
Liechtenstein A I, Katsnelson M I, Antropov V P and Gubanov V A 1987 *J. Magn. Magn. Mater.* **67** 65–74
Liu X B and Altounian Z 2011 *Comput. Mater. Sci.* **50** 841–6
Lukoyanov A V, Kokorina E E, Medvedev M V and Nekrasov I A 2009 *Phys. Rev.* B **80** 104409
Metropolis N, Rosenbluth M, Teller A and Teller E 1953 *J. Chem. Phys.* **21** 1087–92
Miraglia S, Soubeyroux J L, Kolbeck C, Isnard O, Fruchart D and Guillot M 1991 *J. Less-Common Metals* **171** 51–61
Mooij D and Buschow K H J 1988 *J. Less-Common Met.* **136** 207–15
Moruzzi V, Janak J and Williams A 1978 Calculated electronic properties of metals *Calculated Electronic Properties of Metals* (New York: Pergamon)
Okamoto H 2008 *J. Phase Equilib. Diffus.* **29** 116–7
Otani Y, Miyahima H and Chikazumi S 1987 *J. Appl. Phys.* **61** 3436–8
Pastushenkov Y G, Skokov K P, Suponev N P and Stakhovski D 2005 *J. Magn. Magn. Mater.* **290–291** 644–6
Rama Rao K V S *et al* 1999 *Bull. Mater. Sci.* **22** 509–17
Sagawa M 1987 *J. Appl. Phys.* **26** 785–800
Schobinger D *et al* 2002 *J. Magn. Magn. Mater.* **242–245** 1347–9
Seiser B, Drautz R and Pettifor D G 2011 *Acta Mater.* **59** 749–63
Shan-Ho T and Salinas S R 1998 *Braz. J. Phys.* **28** 58–65
Shoemaker C, Shoemaker D and Fruchart F 1984 *Acta Crystallogr.* C **40** 1665
Skomski R 2008 2.4.4 Itinerant antiferromagnets *Simple Models of Magnetism* (Oxford: Oxford University Press) pp 66–71
Steinbeck L, Richter M and Eschrig H 2001 *J. Magn. Magn. Mater.* **226–230** 1011
Sun H, Otani Y and Coey J M D 1992 *J. Magn. Magn. Mater.* **104–107** 1439–40
Swendsen R H and Wang J-S 1987 *Phys. Rev. Lett.* **58** 86–8
Tie-Song Z *et al* 1991 *Phys. Rev.* B **43** 8593–8
Villars P and Cenzual K 2012/13 *Pearson's Crystal Data: Crystal Structure Database for Inorganic Compounds (on CD-ROM)* Release 2012/13 (Materials Park, OH: ASM International)
von Barth U and Hedin L 1972 *J. Phys.C: Solid State Phys.* **5** 1629
Winterlik J *et al* 2012 *Adv. Mater.* **24** 6283–7
Wolfers P, Obbade S, Fruchart D and Verhoef R 1996 *J. Alloys Compounds* **241** 74–9
Wolff U 1989 *Phys. Rev. Lett.* **62** 361
Yousuf M, Sahu P and Rajan K 1986 *Phys. Rev.* B **34** 8086–100
Zhong X-P *et al* 1990 *J. Magn. Magn. Mater.* **86** 333–40